PCCP

PAPER

View Article Online
View Journal | View Issue

Cite this: *Phys. Chem. Chem. Phys.*, 2014, **16**, 19952

The effect of the cation alkyl chain branching on mutual solubilities with water and toxicities†

Kiki A. Kurnia,[a] Tânia E. Sintra,[a] Catarina M. S. S. Neves,[a] Karina Shimizu,[bc] José N. Canongia Lopes,[bc] Fernando Gonçalves,[d] Sónia P. M. Ventura,[a] Mara G. Freire,[a] Luís M. N. B. F. Santos[e] and João A. P. Coutinho*[a]

The design of ionic liquids has been focused on the cation–anion combinations but other more subtle approaches can be used. In this work the effect of the branching of the cation alkyl chain on the design of ionic liquids (ILs) is evaluated. The mutual solubilities with water and toxicities of a series of bis(trifluoromethylsulfonyl)-based ILs, combined with imidazolium, pyridinium, pyrrolidinium, and piperidinium cations with linear or branched alkyl chains, are reported. The mutual solubility measurements were carried out in the temperature range from (288.15 to 323.15) K. From the obtained experimental data, the thermodynamic properties of the solution (in the water-rich phase) were determined and discussed. The COnductor like Screening MOdel for Real Solvents (COSMO-RS) was used to predict the liquid–liquid equilibrium. Furthermore, molecular dynamic simulations were also carried out aiming to get a deeper understanding of these fluids at the molecular level. The results show that the increase in the number of atoms at the cation ring (from five to six) leads to a decrease in the mutual solubilities with water while increasing their toxicity, and as expected from the well-established relationship between toxicities and hydrophobicities of ILs. The branching of the alkyl chain was observed to decrease the water solubility in ILs, while increasing the ILs solubility in water. The inability of COSMO-RS to correctly predict the effect of branching alkyl chains toward water solubility on them was confirmed using molecular dynamic simulations to be due to the formation of nano-segregated structures of the ILs that are not taken into account by the COSMO-RS model. In addition, the impact of branched alkyl chains on the toxicity is shown to be not trivial and to depend on the aromatic nature of the ILs.

Received 26th May 2014,
Accepted 5th August 2014

DOI: 10.1039/c4cp02309a

www.rsc.org/pccp

Introduction

Ionic liquids (ILs) are, by definition, salts with melting temperatures below 100 °C. These organic salts are usually composed of a poorly coordinating, bulky organic cation, and an organic or inorganic anion, which contribute to their low melting points.[1] A special feature of ILs is that their physical and chemical properties, such as density, viscosity, mutual solubilities with water as well as their toxicity, can be easily tuned by an appropriate selection of their constituting ions.[2,3] For example, the solubility of water in 1-butyl-3-methylimidazolium ($[C_4C_1im]$-based-ILs) can be significantly decreased by changing the anion from tetrafluoroborate, $[BF_4]^-$, to bis(trifluoromethylsulfonyl)-imide, $[NTf_2]^-$. In contrast, changing the alkyl chain from $[C_4C_1im][NTf_2]$ to 1-hexyl-3-methylimidazolium bis(trifluoromethylsulfonyl)imide, $[C_6C_1im][NTf_2]$, has a much more limited effect although it also leads to a decrease in the mutual solubilities with water.[4] However, in what concerns the toxicity, the change in the anion has a much smaller impact than the increase in the cation alkyl chain length.[5] These trends suggest that both the cation or the anion of the IL can be molecularly-engineered for specific physico-chemical properties to meet the requirement of a specific application.[6] For a deeper understanding on the design ability of ILs, we have been addressing the effects of the nature of the anion,[7] isomerisation or *quasi* isomerisation,[8]

[a] *Departamento de Química, CICECO, Universidade de Aveiro, 3810-193 Aveiro, Portugal. E-mail: jcoutinho@ua.pt; Fax: +351-234-370084; Tel: +351-234-370200*
[b] *Centro de Química Estrutural, Instituto Superior Técnico, Universidade de Lisboa, 1049-001 Lisboa, Portugal*
[c] *Insituto de Tecnologia Química e Biológica, Universidade Nova de Lisboa, Avenida República, 2780-157 Oeiras, Portugal*
[d] *Departamento de Biologia, CESAM, Universidade de Aveiro, 3810-193 Aveiro, Portugal*
[e] *Centro de Investigação em Química, Departamento de Química e Bioquímica, Faculdade de Ciências da Universidade do Porto, R. Campo Alegre 687, P-4169-007 Porto, Portugal*

† Electronic supplementary information (ESI) available: Experimental data of mutual solubility of ILs and water; fitted parameters from the correlation of the experimental data with eqn (1) and (2); standard thermodynamic molar properties of solution of ILs in water at 298.15 K; Microtox® EC_{50} values (mg L^{-1}) of the studied ILs after 5, 15 and 30 minutes of exposure to the luminescent marine bacteria *Vibrio fischeri*, with the respective 95% confidence limits; studied systems and simulation conditions used for the molecular dynamic simulation; liquid–liquid phase diagram predicted by COSMO-RS. See DOI: 10.1039/c4cp02309a

and the position and size of the alkyl side chain and its symmetry.[8] This work further extends these studies towards the effect of the cation alkyl side chain branching upon the phase behaviour of ionic liquids with water and their toxicities.

The use of hydrophobic ILs, considered here as those not completely miscible with water at temperatures close to room temperature, has shown promising results as media for the recovery of value-added organic compounds from aqueous solutions.[9–12] They may also play an important role in the separation of (bio)alcohols from fermentation broths.[12–16] Conventionally, separating dilute solutions of (bio)alcohols and water requires an extensive distillation, which becomes the most energy intensive step in fuel production.[17] In contrast, using hydrophobic ILs, the phase separation can be achieved at low temperature, facilitating thus the extraction processes with further economic benefits. To design separation processes involving ILs at an industrial scale, there are, at least, two key factors to be considered. First, it is necessary to know a wide range of thermophysical properties, thermodynamic data, and solid–liquid (SLE), liquid–liquid (LLE), and vapour–liquid equilibrium (VLE). Thermophysical properties along with the equilibrium data are also important to get a better understanding on the physicochemical behaviour of ILs and to develop related thermodynamic models.[18–21] Second, when ILs are applied as media for extraction processes from aqueous solutions, they will be in contact with water. Even the most hydrophobic ILs exhibit noticeable solubility in water[4] that must be taken into account due to the fact that most of these ILs are non-biodegradable. Instead, they accumulate in the aquatic ecosystems with potential harmful effects for microorganisms and humans.[22,23] Therefore, in the development of ILs as alternative industrial solvents, the optimisation of technical properties should run in parallel with the minimisation of potential hazards.

In order to evaluate the influence of the IL structure on their toxicity behaviour, an extensive range of ILs has been studied.[24–37] Furthermore, several contributions attempted at understanding the relationship between the ILs toxicity and other properties, such as hydrophobic nature,[38] membrane water partitioning,[39] and lipophilicity.[39,40] Recently, using a large number of ILs, we have shown a close relationship between the ILs toxicity and their solubility in water.[33] The results clearly indicate that the less soluble non-aromatic ILs also exhibit a lower toxicity when compared to aromatic ILs with higher solubility in water.[33] In addition, it was also shown that the distribution of the cation alkyl chains by the two nitrogen atoms in symmetric cations does not seem to have an impact on the toxicity.[33] Nevertheless, a difference in the central atom between the ammonium and phosphonium families does have an impact.[41] In the search for new heuristic rules relating the structure of ILs and their main properties, the use of branched chains is investigated in this work. The advantages of using this solubility–toxicity relationship is that knowledge of solubility can be used to predict their toxicity, or it may prompt design strategies to obtain ILs that exhibit, simultaneously, a low water solubility and toxicity. Thus, this solubility–toxicity relationship may play an important role as these two properties are required in designing ILs as media for the extraction of high-value products from aqueous solutions and fermentation broths.

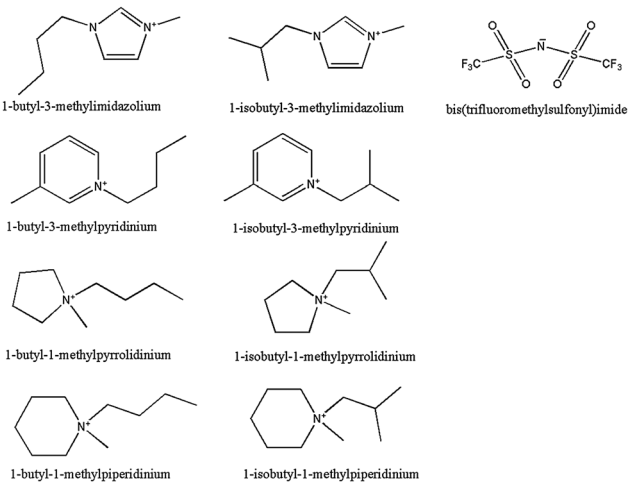

Fig. 1 Chemical structures of the ions constituting the ILs studied in this work.

Based on the concepts expressed above, this work was carried out to investigate the relationship between solubility and toxicity of linear and branched alkyl chains of several families of ILs. For that purpose, we used ILs containing *n*-butyl or iso-butyl (i-butyl) as representatives of linear and branched alkyl chains attached to a cation head group. The ILs studied contain the common bis(trifluoromethylsulfonyl)imide anion combined with imidazolium, pyridinium, piperidinium and pyrrolidinium cations. Fig. 1 depicts the chemical structures of the ions constituting the ILs studied in this work. Herein, the thermodynamic functions of solutions of several ILs in water were determined to develop a molecular insight on how the ions behave in aqueous solution. While the aim of this work is to investigate the relationship between the structure of ILs and their mutual solubility with water and toxicity, the ultimate goal is to draw directions for designing ILs that combine lower solubility in water with a low toxicity. Therefore, the obtained data were analysed by taking into account the structural variation of ILs with their mutual solubilities with water and with their toxicity. In addition, the experimental solubility data were also compared with predictive results from the COnductor like Screening MOdel for Real Solvents (COSMO-RS).[42,43] Aiming to gather a deeper understanding of the underlying mechanism of the IL and/or water solvation phenomena, molecular dynamics simulations have also been performed.

Results and discussion

Mutual solubility with water

The mutual solubilities of the studied ILs with water were determined in the temperature range from 288.15 to 318.15 K and at atmospheric pressure. The novel experimental data on the mutual solubilities along with their respective standard deviations are presented in Table S1 in the ESI.† It is observed that while the mole fraction solubility of ILs in water is in the order of 10^{-4}, the solubility of water in the ILs is much higher, in the 10^{-1}

magnitude. Hence, regardless of the hydrophobic nature of these ILs, it is here shown that they are highly hygroscopic.

The liquid–liquid phase diagrams of all the studied ILs, along with their linear isomers previously reported, are depicted in Fig. 2. The studied binary mixtures of ILs and water exhibit an upper critical solution temperature (UCST) behaviour, as previously observed for other [NTf_2]-based ILs.[4,44] In addition, it is well-known that the hydrogen-bonding interactions occurring between ILs and water are influenced either by the cation or the anion, with the latter having a stronger impact.[7] Looking at the IL-rich region of the phase diagram (*cf.* Fig. 2a), it can be seen that the binary systems containing imidazolium-based ILs exhibit a lower miscibility gap, followed by pyridinium-, pyrrolidinium-, and at last by piperidinium-based ILs. Keeping in mind that the studied ILs have the same alkyl side chains and a common anion, this difference can be interpreted as the result from the contribution of the head groups.

Thus, although in a milder way than the anion, it is here observed that the structure of the cation core also influences the liquid–liquid phase behaviour of IL–water binary systems and can be used to fine-tune the phase diagram.

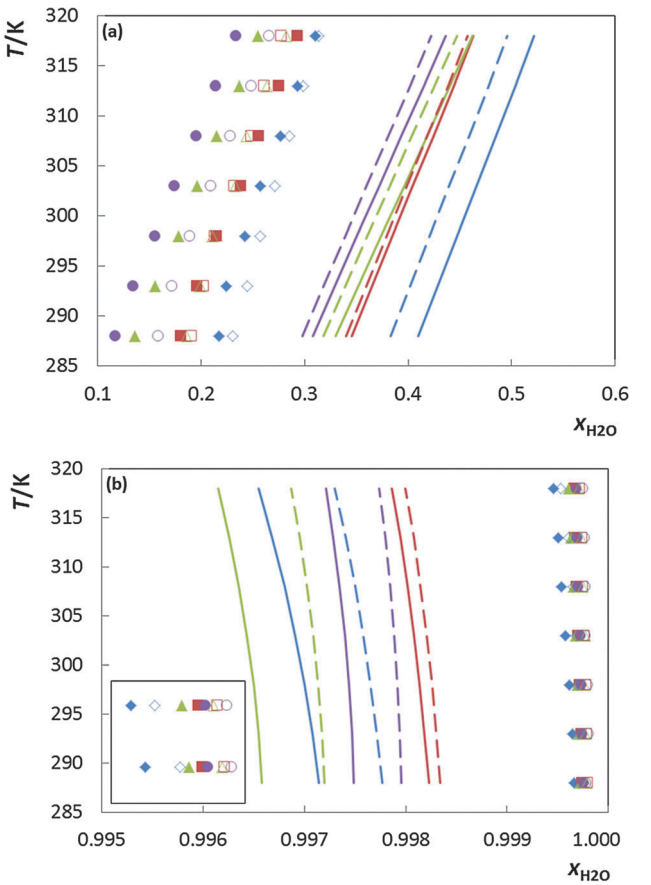

Fig. 2 Liquid–liquid phase diagrams for the binary mixtures composed of water and ILs: (a) IL-rich phase; and (b) water-rich phase. Experimental data (symbols): (◆, ◇) [C_4C_1im][NTf_2]; (■, □) [C_4-3-C_1py][NTf_2]; (▲, △) [C_4C_1pyrr][NTf_2]; and (●, ○) [C_4C_1pip][NTf_2]. The closed and open symbols represent i-butyl and *n*-butyl, respectively. The matching coloured full and dashed lines represent, respectively, the COSMO-RS predictions for the ILs i-butyl and *n*-butyl using the parameterization BP_TZVPD-FINE_C30_1401. The inset presents the experimental ILs solubility in water at 313.15 and 318.15 K.

At the IL-rich phase (*cf.* Fig. 2a) it is observed that water has a higher mole fraction solubility in aromatic-containing head group ILs compared to the non-aromatic fluids. As expected, the aromatic moieties of the head group leads to stronger interactions with water.[45,46] The higher water solubility in the imidazolium- and pyridinium-based ILs, when compared with the pyrrolidinium- and piperidinium-based counterparts, is a result of the more favourable interaction of water with the π systems of those former cations.[7] In addition to the presence of aromatic rings, the water solubility in ILs is also influenced by the number of carbon atoms forming the cation ring. The mutual solubilities of water and hydrophobic ILs are related to their molar volumes as previously shown[44] and as discussed below. Cations with 5 member atoms are thus always more soluble in water than in the 6-member ones. Increasing the number of atoms in the ring leads to an increase in the molar volume, and thus the hydrophobicity of the respective ILs.

Besides these observations, the main goal of this work is to study the effect of linear and branched alkyl chains of ILs upon their mutual solubilities with water. According to the results depicted in Fig. 2a, water has higher solubility in ILs with linear alkyl chains when compared with the solubility in the branched isomers. This behaviour is even more noticeable when the longest aliphatic moiety is attached to a non-aromatic ring. A branched alkyl side chain seems to hinder the accessibility of water to the polar region of the IL, and that leads to a lower solubility of water resulting mainly from steric effects.

At the water-rich phase (Fig. 2b), it is quite interesting to observe that the features of both the head groups and structural isomers are rather different than those observed for the IL-rich phase. Imidazolium-based ILs have the highest solubility in water, followed by pyrrolidinium-, pyridinium-, and eventually piperidinium-based ILs. Peculiarly, a swap is observed between the pyridinium- and pyrrolidinium-based ILs in the water-rich phase. This indicates that the solubility of the ILs in water seems to be primarily controlled by the water cavitation potential of water that is affected by the cation size and, to a lower extent, by their IL aromaticity. For the same reason, the ILs with branched alkyl chains display a slightly higher solubility in the water-rich phase when compared to their linear isomers due to the decrease of the cavitation potential of the branched alkyl chain compared with the linear aliphatic moieties.

Temperature dependence and thermodynamic functions of solution

A simple relationship between solubility *versus* temperature has been obtained. The solubility of water in the IL-rich phase is described by eqn (1), while the solubility of the IL in the water-rich phase is expressed using eqn (2)

$$\ln x_w = A + \frac{B}{T/K} \quad (1)$$

$$\ln x_{IL} = C + \frac{D}{T/K} + E\ln(T/K) \quad (2)$$

where T is the temperature, and A, B, C, D, and E are fitted parameters. Those parameters and their standard deviations are presented in Table S2 in the ESI.† It must be mentioned that in order to apply eqn (1), it is assumed that in the temperature range investigated the change in the standard molar enthalpy of solution of water in the IL phase is negligible. The proposed correlations present a maximum relative deviation to the experimental mole fraction data of 3 and 2%, for the water-rich and IL-rich phases, respectively.

In general, the solubility of ILs in water is very low and can be assumed to be at infinite dilution. Thus, the molar thermodynamic properties of solution, namely the standard molar Gibbs energy, $\Delta_{sol}G^0_m$, the enthalpy, $\Delta_{sol}H^0_m$, and entropy, $\Delta_{sol}S^0_m$, of solution can be derived. These thermodynamic properties are associated with the changes that occur in the solute neighbourhood when one solute molecule is transferred from an ideal gas phase to a diluted ideal solution. Therefore, aiming at exploring the molecular mechanisms behind the solvation phenomenon, the solution standard molar functions were estimated using eqn (3)–(5),[4,8]

$$\Delta_{sol}G^0_m = -RT\ln(x_2)_p \quad (3)$$

$$\frac{\Delta_{sol}H^0_m}{RT^2} = \left(\frac{\partial \ln x_2}{\partial T}\right)_p \quad (4)$$

$$\Delta_{sol}S^0_m = R\left[\frac{\partial(T\ln x_2)}{\partial T}\right]_p \quad (5)$$

where R is the ideal gas constant, p = 0.1 MPa, m refers to molar quantity. These thermodynamic functions for the IL solvation in water at 298.15 K are reported in Table S3 in the ESI.† Since the solubility of water in the IL-rich phase is well above the infinite dilution, the associated thermodynamic molar functions at 298.15 K were not determined.

The positive values for enthalpies of solution indicate that the solubilisation of ILs in water is an endothermic process, thus leading to an UCST-type of phase diagram.[8] The solubility of hydrophobic ILs in water is a hydrophobic hydration, thus dominated by dispersion forces that increase with temperature leading eventually to complete miscibility of the IL in water. Furthermore, in Fig. 3, the molar entropies of a solution of the linear alkyl chain are compared with that of their branched isomers. For ILs with linear alkyl chains, the contribution of approximately -5 J K^{-1} mol^{-1}, per methylene group to the entropy of solution in water was previously demonstrated.[40] The entropy of solutions of ILs with branched alkyl chains are found to be less negative than those of their linear isomers, as depicted in Fig. 3, and it seems that ILs with branched alkyl chains do not follow the same trend. This finding further corroborates the idea that the solvation of branched alkyl chains will lead to an effective lower cavitation volume and potential penalty. That penalty is mostly reflected in the entropy of cavitation that is not as negative as in the linear alkyl chain in about 10 J K^{-1} mol^{-1}.[47] The differentiation between the entropies of solution in all the pairs of isomers are following the trend of $\sim$10 J K^{-1} mol^{-1} of entropy of solution increase between the branched and linear ILs as observed from Fig. 3.

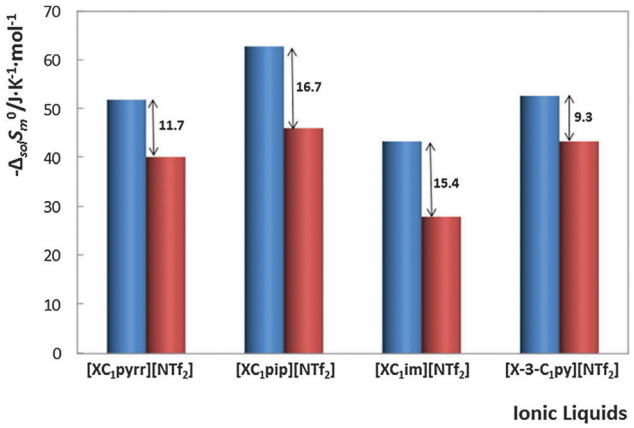

Fig. 3 Entropy of a solution of ILs for linear (blue bars) and branched alkyl chains (red bars) in water at 298.15 K.

The effect of the IL size, in terms of molar volume (see Table S4 in the ESI†) regarding their solubility in water has been investigated. The dependence of the ILs solubility in water with the molar volume of ILs is shown in Fig. 4. The first noticeable result is that the studied ILs with linear alkyl chains fall in the molar volume–solubility correlation line, previously proposed for the linear imidazolium-based ILs.[44] On the other hand, the ILs with branched alkyl chains deviate from that correlation. These results seem to indicate that the solubility of ILs with branched alkyl chains in water is primarily driven by their molar volume that will be directly related by the effective cavitation potential, that is smaller for the branched than for the linear alkyl chains ILs due to the expected favourable shape resulting from the low cavitation surface to volume ratio observed in the branched alkyl chains. Yet the deviations of the branched alkyl chain ILs from the correlation suggest that other phenomena may also be affecting the solubility.

COSMO-RS

Fig. 2 presents the liquid–liquid equilibria for the studied ILs with water. On the IL-rich side (*cf.* Fig. 2a), the same hydrophobic character, considering only the cation core effect, and following the trend [i-C$_4$C$_1$im][NTf$_2$] < [i-C$_4$-3-C$_1$py][NTf$_2$] < [i-C$_4$C$_1$pyrr][NTf$_2$] < [i-C$_4$C$_1$pip][NTf$_2$], was found both for the experimental data and the COSMO-RS predictions. In addition, a similar trend for their linear isomers was also well predicted. Nevertheless, it should be noticed that COSMO-RS fails to predict the difference in the phase behaviour displayed between the linear and branched alkyl chain IL isomers. COSMO-RS always wrongly predicts a higher solubility of water in the ILs with branched alkyl chains. In addition, on the water-rich side (*cf.* Fig. 2b), even though COSMO-RS predicts higher solubility of branched alkyl chains in water than their corresponding linear isomers, the influence of the head group (cation core) is not well described when compared to the experimental data. COSMO-RS predicts a higher solubility of

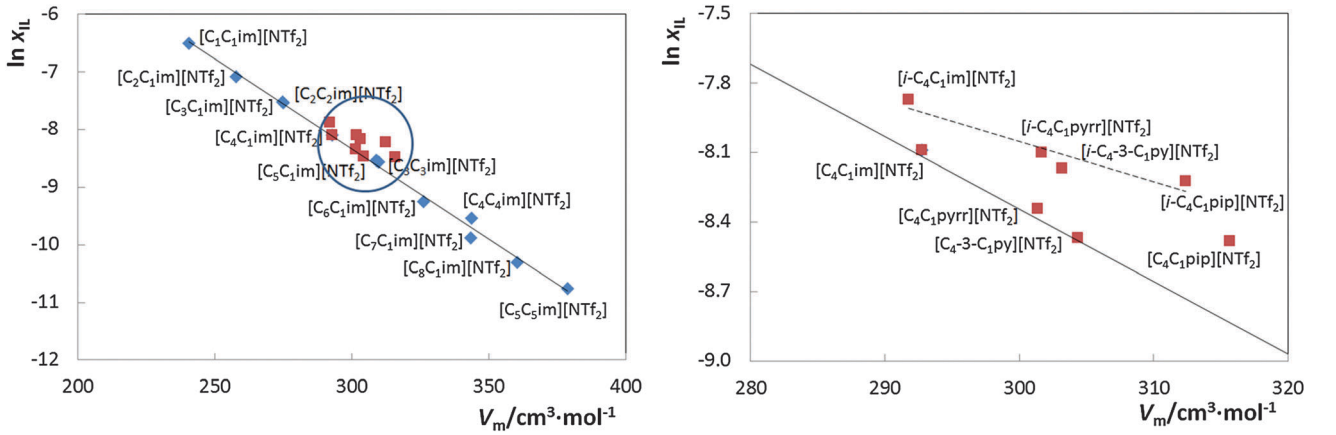

Fig. 4 Solubility of the studied ILs in water (expressed in mole fraction) as a function of the molar volume of ILs. All data are at 298.15 K. The solid lines represent the correlation between the ILs solubility in water and their molar volume taken from density data.[44] The dashed line is only presented to facilitate the interpretation.

the non-aromatic ILs in water (*cf.* Fig. 2b). It should be mentioned that two other COSMO-RS parameterizations were here tested, namely BP_TZVP_C21_0111 and BP_TZVP_C31_1401, and the respective results are given in Fig. S1 and S2 in the ESI.† None of the COSMO-RS parameterizations could correctly describe the differences in behaviour of the water solubility in the ILs between linear and branched alkyl chains. That is no surprise taking into account that in the COSMO-RS simulation box, the weak interaction potential effects like aromatic moieties to water interactions are described based on a simple and empirical interaction potential that is expected to poorly describe the diversity and complexity of the weak interaction potentials between the ILs and water.

Molecular dynamics simulation

In order to understand from a molecular point of view the water solubility data in the isomeric ionic liquids (*n*-butyl *versus* i-butyl alkyl side chains) and to explain the inability of the COSMOS-RS correlations to predict the relative solubility trends on the IL-rich side of the corresponding diagrams, we have performed molecular dynamics (MD) simulations. Three ILs, namely $[C_4C_1im][NTf_2]$ and $[i\text{-}C_4C_1im][NTf_2]$, along with 1-(*n*-propyl)-3-methylimidazolium bis(trifluoromethylsulfonyl) imide, $[C_3C_1im][NTf_2]$, were selected as representative IL systems. Three sets of simulations were then performed: (i) pure ILs, (ii) IL-rich mixtures with water (0.3 mole fraction concentrations of water at 320 K) and (iii) aqueous solutions with the ILs at infinite dilution.

Fig. 5 shows the MD results in terms of the pair radial distribution functions that better describe the interactions between the charged parts of the ILs—the so-called polar network. The figure shows an obvious opposition-of-phase considering the correlations between ions with contrary charge (grey lines) and those of equal sign (red and blue lines). As expected, all three pure ILs show this tell-tale evidence of the presence of a polar network. However, the three IL-rich mixtures with water also show the same pattern. This means that even when the number of water molecules is around one third of those of the IL (before liquid–liquid immiscibility is reached in these systems) the polar network composed of the charged parts of the IL ions still retains most of its interconnectivity. The vertical grid lines superimposed on the $g(r)$ functions of Fig. 5 mark the characteristic wavelength of the periodicity of the polar network in each case. These were calculated from the corresponding structure factor functions also obtained from the MD data. They show that in pure $[C_4C_1im][NTf_2]$, the spacing between the charged components of the polar network (0.725 nm) is slightly larger than in the case of $[C_3C_1im][NTf_2]$ (0.704 nm) (as discussed in previous studies concerning pure 1,3-dialkylimidazolium bis(trifluoromethylsulfonyl)imide ILs with linear tails),[48] whereas for $[i\text{-}C_4C_1im][NTf_2]$, such spacing (0.723 nm) lies closer to that of $[C_4C_1im][NTf_2]$ than to that of $[i\text{-}C_3C_1im][NTf_2]$. These distances can be associated to slightly more compact ($[C_3C_1im][NTf_2]$) or more stretched ($[C_4C_1im][NTf_2]$, $[i\text{-}C_4C_1im][NTf_2]$) polar networks.

When the three IL-rich mixtures are considered it is noticed that all polar networks become more stretched—larger characteristic wavelengths of the periodic behaviour of the corresponding $g(r)$ functions. The values shift from 0.704 to 0.711 nm for $[C_3C_1im][NTf_2]$, from 0.725 to 0.728 nm for $[C_4C_1im][NTf_2]$, and from 0.723 to 0.724 nm in the case of $[i\text{-}C_4C_1im][NTf_2]$. This is in agreement with the fact that the added water molecules will interact mainly with the charged moieties of the ILs (specially the anion), as shown by the water–IL $g(r)$ functions shown in Fig. 6. Other MD works that studied the modification of the IL structure upon addition of water (mainly to hydrophilic ILs)[49] have shown that the water molecules start to surround the polar network causing its swelling and stretching. This is more obvious in the case of $[C_3C_1im][NTf_2]$ since it was the IL with the more compact ionic network.

In conclusion, Fig. 5 and 6 show that the polar networks of all three ILs remain practically unchanged—only slightly swelled—as water molecules start to surround them. In the case of $[C_3C_1im][NTf_2]$, more water molecules can be accepted around its polar network (hence the slightly larger solubility of water in $[C_3C_1im][NTf_2]$ relative to that of $[C_4C_1im][NTf_2]$ or $[i\text{-}C_4C_1im][NTf_2]$) because

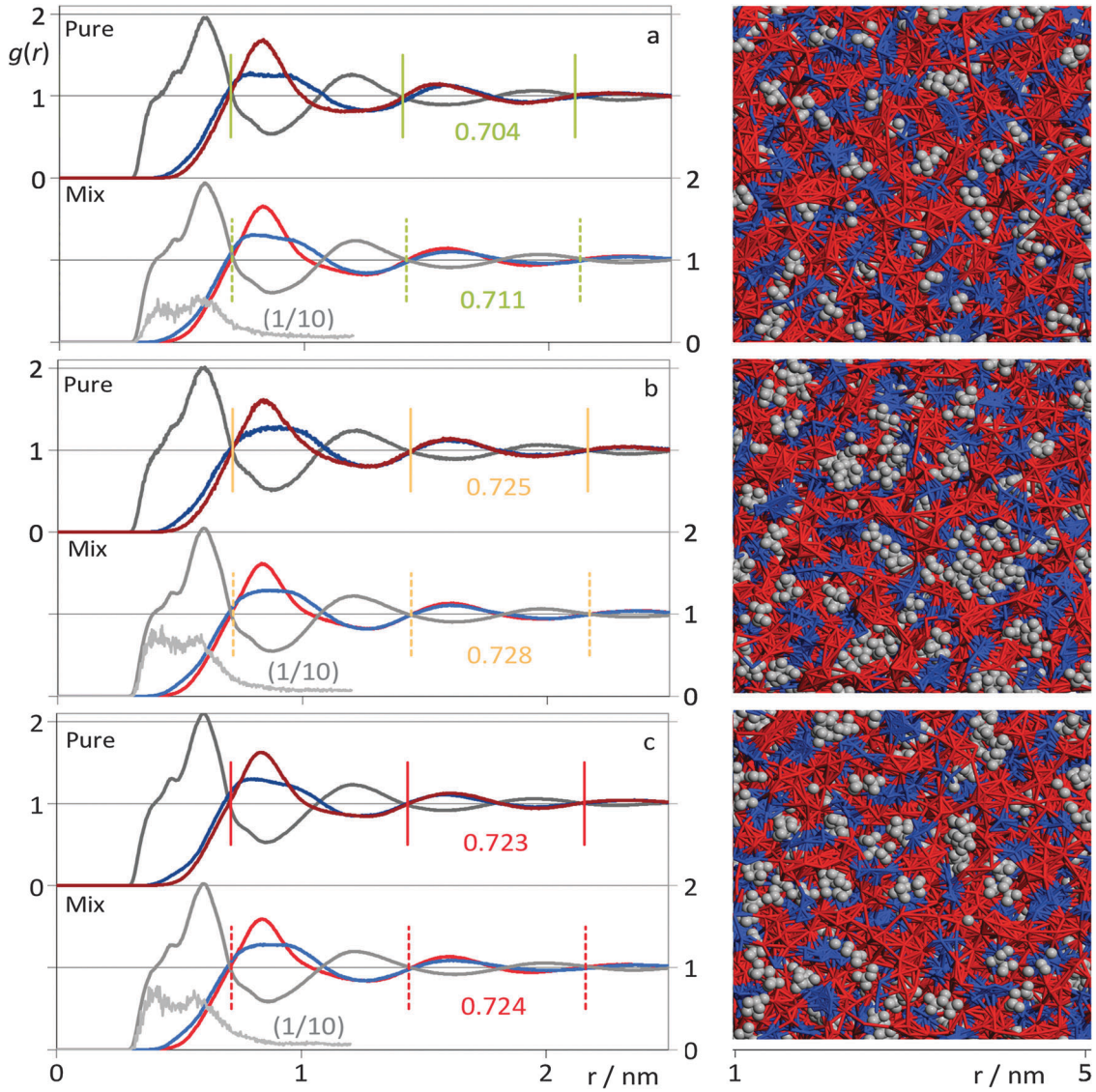

Fig. 5 Molecular dynamic data for 1-alkyl-3-methylimidazolium-based ILs with (a) propyl, (b) butyl, and (c) iso-butyl side chains. The graphs on the left are the radial distribution functions between the centroid of the imidazolium ring, CM, and the nitrogen atom, NBT, of the anion: CM–NBT in gray; NBT–NBT in red; and CM–CM in blue. ''Pure'' and ''Mix'' refer to simulations in the neat ILs and in IL mixtures containing 0.3 mole fraction of water (or at IL infinite dilution for the lines labeled 1/10). The colored vertical gridlines correspond to the characteristic d-spacing given by $2\pi/q$ of the structure factor intermediate q-peak. The images on the right are simulation box snapshots for the three pure ionic liquids: charged parts of the cation in blue, charged parts of the anion in red, alkyl side chains (C2 to CT) in gray.

it can swell more its polar network (it is more interconnected and occupies a larger volume fraction in the pure IL). On the other hand, the difference between the solubilities of water in $[C_4C_1im][NTf_2]$ and $[i\text{-}C_4C_1im][NTf_2]$ cannot be explained by any meaningful difference between the polar networks of the two ILs.

Fig. 7 shows the correlation functions between the terminal carbon atoms in the three pure ILs (*cf.* Fig. 7a) and the three IL–water mixtures (*cf.* Fig. 7b). The first peaks point to the existence of small tail-to-tail alkyl clusters in the midst of the polar network. As shown in previous studies,[48,50] such peaks increase along the $[C_nC_1im][NTf_2]$ homologous series, indicating the enlargement of the clusters, and reach a plateau around $n = 5$ that signals the coalescence of the clusters and the formation of a continuous non-polar domain. The point to take into consideration at this stage is that, whereas the polar network of $[i\text{-}C_4C_1im][NTf_2]$ is much more similar to that of $[C_4C_1im][NTf_2]$ than to that of $[C_3C_1im][NTf_2]$, the non-polar clusters of $[i\text{-}C_4C_1im][NTf_2]$ show correlations lower than those of $[C_3C_1im][NTf_2]$ (*cf.* Fig. 7a). In terms of segregation of those clusters in the midst of the polar network this means that the end carbons of the $[C_4C_1im][NTf_2]$ chains are much more effectively segregated from the polar network than their $[i\text{-}C_4C_1im][NTf_2]$ counterparts. The situation is intensified when water is added to the IL (*cf.* Fig. 7b): the first peak of the CT–CT correlation in the $[C_4C_1im][NTf_2]$–water mixture increases whereas the same peak for the $[i\text{-}C_4C_1im][NTf_2]$–water mixture

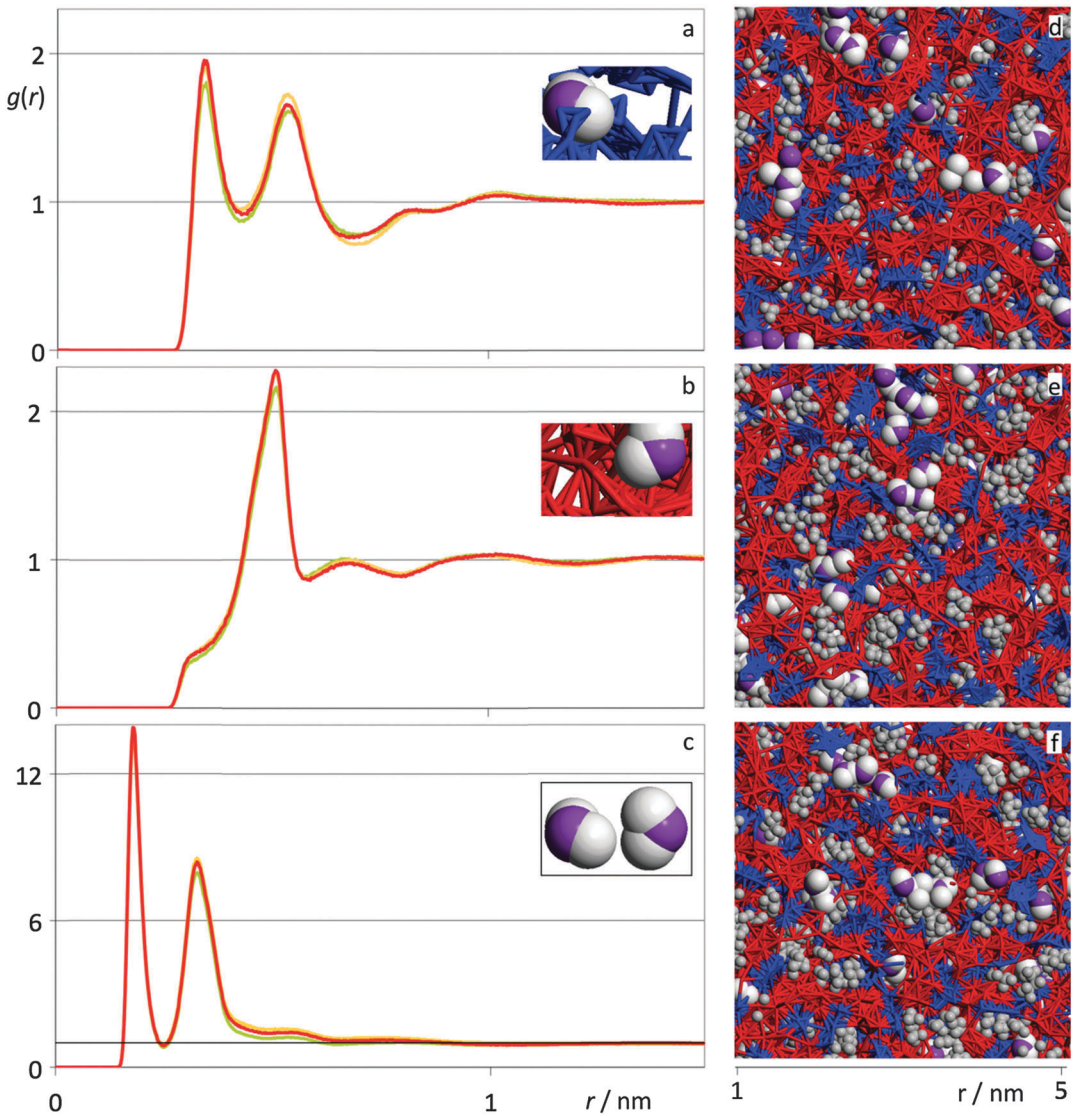

Fig. 6 Radial distribution functions in IL mixtures with 0.3 water mole fraction, between the oxygen atom of water, OW, and: (a) the carbon atom of the imidazolium ring lying between the two nitrogen atoms, CR; (b) NBT; and (c) OW. The lines for the three types of IL analyzed are practically superimposed (green for $[C_3C_1im][NTf_2]$, yellow for $[C_4C_1im][NTf_2]$ and red for $[i\text{-}C_4C_1im][NTf_2]$). (d–f) Simulation box snapshots for the three ionic liquid mixtures: (d) $[C_3C_1im][NTf_2]$; (e) $[C_4C_1im][NTf_2]$; and (f) $[i\text{-}C_4C_1im][NTf_2]$. Colors as in figure MD1, water molecules in purple/white.

remains the same. In other words the linear nature of the alkyl chains of $[C_4C_1im][NTf_2]$ allows them to form non-polar clusters that keep the corresponding end-carbon atoms further away from the polar network than the end-carbon atoms of their ramified counterparts. In $[i\text{-}C_4C_1im][NTf_2]$ the alkyl clusters remain closer to the polar network, thus partially hindering the interaction of the latter with water in agreement with the conclusion derived from the experimental solvation thermodynamics. The striking difference between Fig. 7a and b (showing the effective non-polar cluster segregation when water is added to $[C_4C_1im][NTf_2]$ and the absence of a similar effect in $[i\text{-}C_4C_1im][NTf_2]$) explains the solubility differences experimentally observed and already discussed from a phenomenological point of view in the corresponding sub-section. It must be stressed that $[C_3C_1im][NTf_2]$ behaves like $[i\text{-}C_4C_1im][NTf_2]$ but its solubility is higher due to a larger volume fraction occupied by its polar network.

The inability of the COSMO-RS correlations to predict the relative solubility of water in $[C_4C_1im][NTf_2]$ and $[i\text{-}C_4C_1im][NTf_2]$ could also be related to a subtle difference in the way the nano-segregated structure of the ILs (polar network interspersed with non-polar domains) interferes with the interactions between the water solute and the most interactive centres of the IL located at the charged parts of the ions.

On the water-rich side of the mixtures (when small amounts of IL solute are added to water) it is much harder to obtain statistical meaningful results using MD simulations. Nevertheless, we have performed simulations containing a single ionic pair and a few hundreds of water molecules in order to analyse the main structural features of solutions with the IL

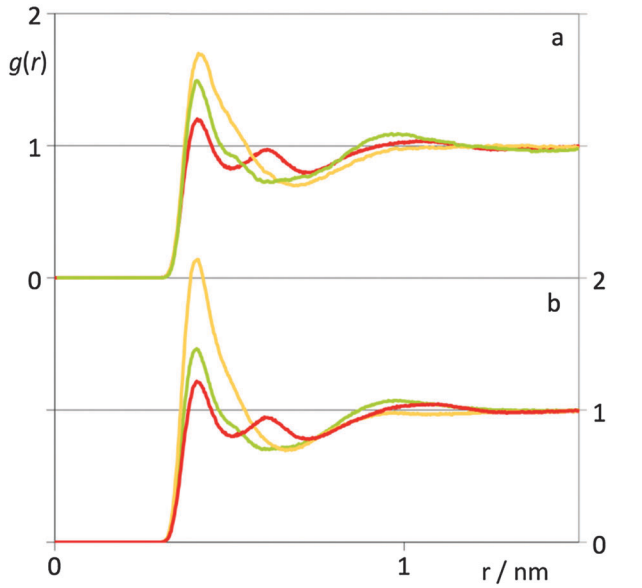

Fig. 7 Radial distribution functions in (a) pure ILs and in (b) IL mixtures with 0.3 water mole fraction, between the terminal carbon atoms of the alkyl chains, CT. Green = $[C_3C_1im][NTf_2]$, yellow = $[C_4C_1im][NTf_2]$ and red = $[i\text{-}C_4C_1im][NTf_2]$.

under infinite-dilution-like conditions. The main point to be noticed is that the anion–cation correlation functions (also presented in Fig. 5 with 1/10 magnification) show that the two ions form ion pairs more often, and for longer times than what would be expected if they were completely isolated and solvated by water molecules and encountered each other on a purely random basis. This suggests the tendency of these ions to form a second IL-rich liquid phase as soon as their concentration is raised above their (very low) solubility limit in water. In a previous work,[4] it was shown that the solubility in water follows the order of $[C_3C_1im][NTf_2] > [C_4C_1im][NTf_2]$. If ion pairs are the prevalent solvated species in the midst of the aqueous solution, this means that solubility in the water-rich side is dominated by the hydrophobic effects stemming from the alkyl chains protruding from the ion pair. Such effect is bigger in $[C_4C_1im][NTf_2]$ and leads to a lower solubility limit ($x_{IL} = 3.1 \times 10^{-4}$) than that from $[C_3C_1im][NTf_2]$ ($x_{IL} = 5.4 \times 10^{-4}$). The more compact alkyl side chain of $[i\text{-}C_4C_1im][NTf_2]$ (it does not protrude so much as that of $[C_4C_1im][NTf_2]$ and stays closer to the ion pair) does not have the detrimental effect observed for the IL-rich side (water is surrounding the whole ion pair anyway) and contributes to a lower hydrophobic effect and hence to a larger solubility ($x_{IL} = 3.8 \times 10^{-4}$) than that observed for $[C_4C_1im][NTf_2]$.

Microtox® toxicity tests

The growing awareness of the environmental issues associated with IL applications has spurred the research on "greener", biodegradable and biocompatible ILs. The standard assays using the luminescent marine bacteria *Vibrio fischeri* is nowadays one of the most widespread toxicological bioassays due to its quick response, simplicity and cost-effective implementation. There have been attempts at understanding the biological impact of the cation alkyl side chain length,[34] the anion,[40] the cation core,[34,51] the aromatic nature,[51] and the central atom of the cation[41] of the ILs on their (eco)toxicological profile. Those results suggest that the presence of branched chains may also be relevant to the toxicity of ILs. Thus, in this work, the impact of branched and linear[34] alkyl chains of a wide set of ILs, toward their toxicity against luminescent bacteria *Vibrio fischeri* was investigated.

Table S5 in the ESI† presents the EC_{50} results for all the ILs studied against the luminescent bacteria *Vibrio fischeri* at exposure times of 5, 15 and 30 minutes. The EC_{50} values obtained clearly show that the studied ILs can be divided into two main groups, as depicted in Fig. 8: (i) the non-aromatic, represented by the pyrrolidinium and piperidinium families; and (ii) the aromatic groups represented by the imidazolium and pyridinium cations, which exhibit a different behaviour when branched alkyl chains are present. Two distinct behaviours are therefore identified. The first one, for the aromatic ILs with the branched isomers exhibiting lower toxicity,[34] and the second one for the non-aromatic ILs and where the branched isomers exhibit a higher toxic nature when compared with the linear ones. Thus, these results suggest that it is possible to manipulate the biological impact of ILs by incorporating branched chains on the cation and that their influence on the ecotoxicity is dependent on the IL's aromatic *vs.* non-aromatic nature. However, the presence of branched chains does not influence the effect previously described[33] where 6-member rings are always more toxic than the 5-member ring cation ILs.

The relationship between the toxicities and the solubility of these ILs in water is depicted in Fig. 9. The results indicate a linear relationship between the EC_{50} values and the solubility of ILs in water, including the aromatics and the isomeric ILs. However, the non-aromatic ILs studied do not follow this regular trend, suggesting that the toxicity of this set of ILs is not only governed by their hydrophobic or aromatic/non-aromatic nature.

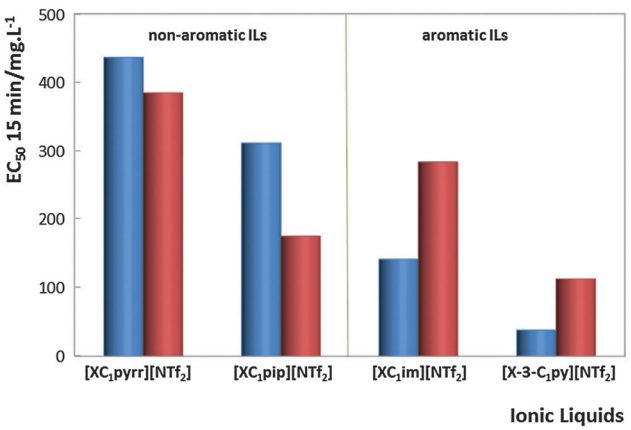

Fig. 8 Effect of the ILs structural isomerism on their toxicity as a function of their aromatic/non-aromatic nature for linear (blue bars) and branched alkyl chains (red bars).

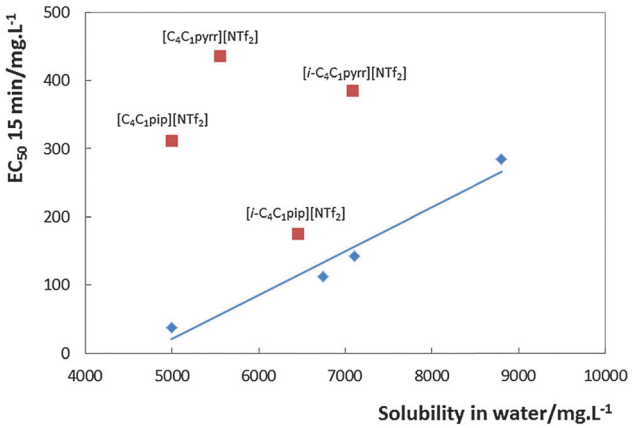

Fig. 9 Correlation between the EC_{50} values at 15 minutes of exposure and the solubility of the respective ILs in water (EC_{50}/mg L^{-1} = 0.0645/mg L^{-1} – 301.82, R^2 = 0.9603). The solubility data for [C_4C_1im][NTf_2],[4] [C_4C_1pyrr][NTf_2],[45] and [C_4-3-C_1py][NTf_2].[8] All data are at 298.15 K. Symbols: (♦), aromatic ILs, and (■), non-aromatic ILs.

Conclusions

The knowledge of the mutual solubility of ILs with water and their toxicity towards aquatic organisms is important in their design as media for the extraction of high-value compounds from aqueous solutions. The chemical structures of ILs have an impact on their mutual solubility and toxicity. In this work, we have reported, for the first time, the mutual solubilities with water and the toxicity of ILs with branched alkyl chains, and compared these results with their isomeric and linear counterparts. In this work, we have reported, for the first time, the impact of branching alkyl chains of ILs toward their mutual solubility with water and their toxicity against luminescent bacteria *Vibrio fischeri*.

Aromatic and non-aromatic ILs were studied, namely imidazolium-, pyridinium-, pyrrolidinium-, and piperidinium-based compounds. In general, it was observed that increasing from five to six carbon atoms in the central cation ring, regardless of the aromatic/non-aromatic nature of the ILs, leads to a reduction in the solubility in water and to an increase in their toxicity. It was also observed that the aromatic nature of the IL plays an important role in the solubility of water in the ILs. The water solubility in linear and branched alkyl chain ILs was further rationalized using MD simulation and the results highlighted the differences in the formation of nano-segregated structures in ILs. On the other hand, the solubility of ILs in water is primarily dictated by their molecular volume and shape. The solubility of ILs with branched alkyl chains in water is significantly different from their linear isomers. This finding is further supported by the thermodynamic analysis, along with the inability of COSMO-RS to correctly predict the differences between branched and linear alkyl chains. The solubility of ILs with branched alkyl chains in water is driven by higher entropy of the solution that seems to be associated to a lower effective volume and potential of cavitation in water. While the branched alkyl chain ILs exhibited higher solubility in water than their linear isomers, their impact on the toxicity is dependent on the aromatic nature of the cation. The toxicity of branched alkyl chains attached to the aromatic ring of ILs is lower than that of their linear isomers, whereas the opposite trend was observed for the non-aromatic ring ILs. This behaviour may indicate that the toxicity of the set of ILs here studied is not only governed by the ILs' hydrophobic or aromatic/non-aromatic nature, but other factors may be present, yet to be discovered.

Experimental procedure

Chemicals

The ILs used in this work are constituted by the common bis(trifluoromethylsulfonyl)imide anion combined with the following cations: 1-(i-butyl)-3-methylimidazolium, [i-C_4C_1im][NTf_2]; 1-(*n*-butyl)-3-methylpyridinium, [C_4-3-C_1py][NTf_2]; 1-(i-butyl)-3-methylpyridinium, [i-C_4-3-C_1py][NTf_2]; 1-(*n*-butyl)-1-methylpyrrolidinium, [C_4C_1pyrr][NTf_2]; 1-(i-butyl)-1-methylpyrrolidinium, [i-C_4C_1pyrr][NTf_2]; 1-(*n*-butyl)-1-methylpiperidinium, [C_4C_1pip][NTf_2]; and 1-(i-butyl)-1-methylpiperidinium, [i-C_4C_1pip][NTf_2]. All ILs were acquired from Iolitec. Prior to the experimental measurements, individual samples of all ILs were dried under vacuum at 0.1 Pa and 353.15 K under constant stirring for a minimum period of 48 h. The purity of each IL was further checked by ^{1}H, ^{13}C, and ^{19}F NMR. All samples displayed purities higher than >99 wt%. The water content of the dried ILs was determined using a Metrohm 831 Karl Fischer (KF) coulometer, with the analyte Hydranal® – Coulomat AG from Riedel-de Haën, and was found to be below 100 ppm for all samples. Ultrapure water, double distilled, passed through a reverse osmosis system and further treated with a MilliQ plus 185 water purification apparatus, was used throughout the mutual solubility experiments. The water used exhibits a resistivity of 18.2 MΩ cm, a TOC smaller than 5 μg dm^{-3} and is free of particles >0.22 μm.

Mutual solubility measurements

The mutual solubilities between water and ILs were determined in the temperature range from (288.15 to 318.15) K and at atmospheric pressure using an experimental procedure previously detailed.[4,7,8,46] The samples of the binary mixtures of ILs and water were put in tightly-closed glass vials with a septum cap. The samples were then vigorously stirred and allowed to settle and equilibrate inside an aluminium block, specially designed for this purpose, for at least 48 h. This period of time proved to be enough to guarantee a complete separation of the two phases, as well as their saturation.[52] The aluminium block was placed in an isolated air bath capable of maintaining the temperature within ±0.01 K. The temperature control was achieved using a PID temperature controller driven by a calibrated Pt100 (class 1/10) temperature sensor inserted into the aluminium block. A Julabo (model F25-HD) refrigerated bath and circulator was used as a cooling source. Both phases were sampled at each temperature from the equilibrium vials using glass syringes maintained dry and kept at the same temperature of the measurements.

The solubility of water in the IL-rich phase was measured by KF titration. Approximately 0.1 g of the IL-rich phase was sampled and directly injected in the KF coulometric titrator to determine the water content. The solubility of aromatic ILs, [i-C_4C_1im][NTf_2] and [i-C_4-3-C_1py][NTf_2], in the water-rich phase was determined by UV-Vis spectroscopy, using a SHIMADZU UV-1700 PharmaSpec Spectrometer. For the water-rich phase, *ca.* 0.5 g of each sample was taken and diluted in (250–500) cm^3 of ultrapure water. The quantifications were carried out at λ = 211 nm and λ = 266 nm, which are the maximum absorption wavelengths found for [i-C_4C_1im][NTf_2] and [i-C_4-3-C_1py][NTf_2], respectively.

The solubility of non-aromatic ILs was determined by a conductivity method previously described.[45,46] The conductivity of the solution was measured using a Mettler Toledo S47 SevenMulti™ dual pH/conductivity meter, coupled with an inLab®741 Conductivity Probe as electrode. The samples of the water-rich phase were weighted and further diluted in ultra-pure water in a ratio of 1 : 20. Previous optimization tests regarding the appropriate dilution were carried out aiming at obtaining significant conductivity values and within the equipment higher accuracy.

Prior to the determination of the IL content in the water-rich phase, calibration curves were performed for each IL and in an adequate concentration range. Each stock solution was prepared gravimetrically within $\pm 10^{-5}$ g and at least 2 calibration curves were determined for each IL to confirm that no gravimetric errors occurred during the preparation of the stock solutions.

Each measurement was repeated at least 5 times, and the results are reported as the average solubility value along with the respective standard deviations.

COSMO-RS

The COnductor-like Screening MOdel for Real Solvents (COSMO-RS) is based on quantum chemical calculations and can be used to predict the thermodynamic properties of fluid mixtures. COSMO-RS is a novel and efficient method for the *a priori* prediction of thermophysical data and has been developed in 1994. The details about the COSMO-RS are described in the literature.[42,53] Previously we used COSMO-RS to predict the equilibrium behaviour of ILs and water and already confirmed its capability as a predictive tool.[7,46]

The standard procedure of COSMO-RS to predict the phase behaviour between ILs and water used in this work consists of two main steps. In the first step, the continuum solvation COSMO calculations of electronic density and molecular geometry were performed using the TURBOMOLE 6.4 program package at the BP-TZVPD-FINE level, introduced in 2012. These calculations are based on a Turbomole BP-RI-DFT COSMO single point calculation with the TZVPD basis set on top of an optimized BP/TZVP/COSMO geometry. The COSMO single point calculation consists of a TZVPD basis set with diffuse basis functions and a novel type of molecular surface cavity construction (fine grid marching tetrahedron cavity, FINE).[54] It creates a COSMO surface whose segments are more uniform and evenly distributed compared to the standard COSMO cavity. The gas phase energy files of this level are optimized on Turbomole on the BP-RI-DFT level with the TZVP basis set, followed by a single point BP-RI-DFT calculation with the TZVPD basis set. In the second step, the estimation of the phase diagrams of binary mixtures of ILs and water was carried out using the COSMOtherm program using the parameter file BP_TZVP_C30_0140 (COSMOlogic GmbH & Co KG, Leverkusen, Germany).[55] The detailed calculation of the phase equilibrium using COSMOtherm is explained in our previous work.[56] In all calculations, the ILs were always treated as isolated ions at the quantum chemical level. In a previous work,[57] the best predictions of the experimental data were obtained with the lowest energy conformations or with the global minimum for both cation and anion. Thus, in this work, the lowest energy conformations of all the species involved were used in the COSMO-RS calculations.

Molecular dynamics simulations

Molecular dynamics (MD) simulations of phases of different pure ionic liquids ([C_3C_1im][NTf_2], [C_4C_1im][NTf_2] and [i-C_4C_1im][NTf_2]) and their aqueous mixtures were carried out using the DLPOLY package.[58] Water and all ILs were modelled using, respectively, the SPC model[59] and a previously described all atom force field (CL&P),[60–62] which is based on the OPLS-AA framework,[63] but was to a large extent developed specifically to encompass entire IL families. For each mixture, we started from low-density initial configurations composed either of 1 ion pair and 600 water molecules or 300 IL ion pairs and 130 water molecules. For pure ILs, the configuration for 1-(*n*-propyl)-1-methylimidazolium bis-(trifluoromethylsulfonyl)-imide, [C_3C_1im][NTf_2], and [C_4C_1im][NTf_2] was a previously equilibrated system from an earlier simulation study of the bulk liquid[48,64,65] and for [i-C_4C_1im][NTf_2] we also started from low-density configurations composed of 300 ion pairs. The number of ion pairs and size of the box for all ILs and their aqueous mixtures are presented in Table S6 in the ESI.† The boxes were equilibrated under isothermal–isobaric ensemble conditions for 1 ns at 318 K and 1 atm using the Nosé–Hoover thermostat and isotropic barostat with time constants of 0.5 and 2 ps, respectively. Several consecutive simulation runs of 1 ns each (at least four in the case of IL-rich mixtures and at least eight in the case of water-rich mixtures), were used to produce equilibrated systems at the studied temperature. Electrostatic interactions were treated using the Ewald summation method considering six reciprocal-space vectors, and repulsive–dispersive interactions were explicitly calculated below a cut-off distance of 1.6 nm (long-range corrections were applied assuming the system has a uniform density beyond that cut-off radius).

Standard Microtox® liquid-phase assays

To evaluate the impact of branched alkyl chains on the ecotoxicity of ILs, several Standard Microtox® liquid-phase assays were carried out. Microtox® was used to evaluate the inhibition of the *Vibrio fischeri* (strain NRRL B-11177) luminescence followed by its exposure to each IL solution. The indications of the manufacturer on the standard 81.9 test protocol were followed.[66] The bacteria was exposed to a range of diluted aqueous solutions relative to the previously prepared stock solution, with a known concentration (0–81.9 wt%) of each IL. After 5, 15, and 30 minutes of exposure to each IL aqueous

solution, the bacterial bioluminescence emission of *Vibrio fischeri* was measured and compared with the bioluminescence emission of a blank control sample. The corresponding 5 min-, 15 min- and 30 min-EC_{50} values (estimated concentration yielding a 50% of inhibition effect) were evaluated through the Microtox® Omni™ software version 4.1.[66] The EC_{50} values, plus the corresponding 95% confidence intervals, were estimated for each IL tested by non-linear regression, using the least-squares method to fit the data to the logistic equation.

Acknowledgements

This work was financed by national funding from Fundação para a Ciência e a Tecnologia (FCT, Portugal), European Union, QREN, FEDER and COMPETE by the projects PEST-C/CTM/LA0011/2013, PEST-C/EQB/LA0020/2013, PEST-OE/QUI/UI0100/2013, PTDC/AAC-AMB/119172/2010 and FCT-ANR/CTM-NAN/0135/2012 (including a post-doctoral grant of K.S.). The authors also thank FCT for the doctoral and post-doctoral grants SFRH/BD/70641/2010, SFRH/BPD/79263/2011, SFRH/BD/85871/2012, SFRH/BPD/88101/2012 of C. M. S. S. Neves, S. P. M. Ventura, T. E. Sintra, and K. A. Kurnia, respectively. M. G. Freire acknowledges the European Research Council (ERC) for the Grant ERC-2013-StG-337753.

References

1 P. Wasserscheid and T. Welton, *Ionic Liquids in Synthesis*, Wiley-VCH Verlag GmbH & Co. KGaA, Darmstadt, Federal Republic of Germany, 2nd edn, 2009, vol. 1.
2 N. V. Plechkova and K. R. Seddon, *Ionic Liquids Uncoiled – Critical Expert Overviews*, A John Wiley & Sons, Inc., Publication, 2013.
3 M. G. Freire, A. F. M. Cláudio, J. M. M. Araújo, J. A. P. Coutinho, I. M. Marrucho, J. N. C. Lopes and L. P. N. Rebelo, *Chem. Soc. Rev.*, 2012, **41**, 4966.
4 M. G. Freire, P. J. Carvalho, R. L. Gardas, I. M. Marrucho, L. M. N. B. F. Santos and J. A. P. Coutinho, *J. Phys. Chem. B*, 2008, **112**, 1604.
5 D. J. Couling, R. J. Bernot, K. M. Docherty, J. K. Dixon and E. J. Maginn, *Green Chem.*, 2006, **8**, 82.
6 J. Brennecke and E. J. Maginn, *AIChE J.*, 2001, **47**, 2384.
7 M. G. Freire, C. M. S. S. Neves, P. J. Carvalho, R. L. Gardas, A. M. Fernandes, I. M. Marrucho, L. M. N. B. F. Santos and J. A. P. Coutinho, *J. Phys. Chem. B*, 2007, **111**, 13082.
8 M. G. Freire, C. M. S. S. Neves, K. Shimizu, C. E. S. Bernardes, I. M. Marrucho, J. A. P. Coutinho, J. N. Canongia Lopes and L. P. N. Rebelo, *J. Phys. Chem. B*, 2010, **114**, 15925.
9 D. Rabari and T. Banerjee, *Fluid Phase Equilib.*, 2013, **355**, 26.
10 S. E. Davis and S. A. Morton Iii, *Sep. Sci. Technol.*, 2008, **43**, 2460.
11 G. Severa, G. Kumar, M. Troung, G. Young and M. J. Cooney, *Sep. Purif. Technol.*, 2013, **116**, 265.
12 L. D. Simoni, A. Chapeaux, J. F. Brennecke and M. A. Stadtherr, *Comput. Chem. Eng.*, 2010, **34**, 1406.
13 R. P. Swatloski, A. E. Visser, W. M. Reichert, G. A. Broker, L. M. Farina, J. D. Holbrey and R. D. Rogers, *Green Chem.*, 2002, **4**, 81.
14 V. Najdanovic-Visak, L. P. N. Rebelo and M. Nunes da Ponte, *Green Chem.*, 2005, **7**, 443.
15 A. Chapeaux, L. D. Simoni, T. S. Ronan, M. A. Stadtherr and J. F. Brennecke, *Green Chem.*, 2008, **10**, 1301.
16 X. Hu, J. Yu and H. Liu, *J. Chem. Eng. Data*, 2006, **51**, 691.
17 N. Qureshi, S. Hughes, I. S. Maddox and M. A. Cotta, *Bioprocess Biosyst. Eng.*, 2005, **27**, 215.
18 T. Banerjee, M. K. Singh, R. K. Sahoo and A. Khanna, *Fluid Phase Equilib.*, 2005, **234**, 64.
19 A. Haghtalab and P. Mahmoodi, *Fluid Phase Equilib.*, 2010, **289**, 61.
20 Z. Lei, C. Dai, X. Liu, L. Xiao and B. Chen, *Ind. Eng. Chem. Res.*, 2012, **51**, 12135.
21 Z. Lei, J. Zhang, Q. Li and B. Chen, *Ind. Eng. Chem. Res.*, 2009, **48**, 2697.
22 K. S. Egorova and V. P. Ananikov, *ChemSusChem*, 2014, **7**, 336.
23 T. P. Thuy Pham, C.-W. Cho and Y.-S. Yun, *Water Res.*, 2010, **44**, 352.
24 K. D. Weaver, H. J. Kim, J. Sun, D. R. MacFarlane and G. D. Elliott, *Green Chem.*, 2010, **12**, 507.
25 M. H. Fatemi and P. Izadiyan, *Chemosphere*, 2011, **84**, 553.
26 M. McLaughlin, M. J. Earle, M. A. Gilea, B. F. Gilmore, S. P. Gorman and K. R. Seddon, *Green Chem.*, 2011, **13**, 2794.
27 X. Wang, C. A. Ohlin, Q. Lu, Z. Fei, J. Hu and P. J. Dyson, *Green Chem.*, 2007, **9**, 1191.
28 A. Garcia-Lorenzo, E. Tojo, J. Tojo, M. Teijeira, F. J. Rodriguez-Berrocal, M. P. Gonzalez and V. S. Martinez-Zorzano, *Green Chem.*, 2008, **10**, 508.
29 C. W. Cho, Y. C. Jeon, T. P. T. Pham, K. Vijayaraghavan and Y. S. Yun, *Ecotoxicol. Environ. Saf.*, 2008, **71**, 166.
30 S. P. M. Ventura, R. L. Gardas, F. Gonçalves and J. A. Coutinho, *J. Chem. Technol. Biotechnol.*, 2011, **86**, 957.
31 X. D. Hou, Q. P. Liu, T. J. Smith, N. Li and M. H. Zong, *PLoS One*, 2013, **8**(3), e59145, DOI: 10.1371/journal.pone.0059145.
32 S. P. M. Ventura, A. M. M. Gonçalves, F. Gonçalves and J. A. P. Coutinho, *Aquat. Toxicol.*, 2010, **96**, 290.
33 S. P. M. Ventura, A. M. M. Gonçalves, T. Sintra, J. L. Pereira, F. Gonçalves and J. A. P. Coutinho, *Ecotoxicology*, 2013, **22**, 1.
34 S. P. M. Ventura, C. S. Marques, A. A. Rosatella, C. A. M. Afonso, F. Gonçalves and J. A. P. Coutinho, *Ecotoxicol. Environ. Saf.*, 2012, **76**, 162.
35 C. Pretti, C. Chiappe, D. Pieraccini, M. Gregori, F. Abramo, G. Monni and L. Intorre, *Green Chem.*, 2006, **8**, 238.
36 C. Pretti, C. Chiappe, I. Baldetti, S. Brunini, G. Monni and L. Intorre, *Ecotoxicol. Environ. Saf.*, 2009, **72**, 1170.
37 C. Pretti, M. Renzi, S. Ettore Focardi, A. Giovani, G. Monni, B. Melai, S. Rajamani and C. Chiappe, *Ecotoxicol. Environ. Saf.*, 2011, **74**, 748.
38 J. Salminen, N. Papaiconomou, R. A. Kumar, J.-M. Lee, J. Kerr, J. Newman and J. M. Prausnitz, *Fluid Phase Equilib.*, 2007, **261**, 421.

39 S. Stolte, J. Arning, U. Bottin-Weber, A. Muller, W.-R. Pitner, U. Welz-Biermann, B. Jastorff and J. Ranke, *Green Chem.*, 2007, **9**, 760.
40 M. Matzke, S. Stolte, K. Thiele, T. Juffernholz, J. Arning, J. Ranke, U. Welz-Biermann and B. Jastorff, *Green Chem.*, 2007, **9**, 1198.
41 P. J. Carvalho, S. P. M. Ventura, M. L. S. Batista, B. Schröder, F. Gonçalves, J. Esperança, F. Mutelet and J. A. P. Coutinho, *J. Chem. Phys.*, 2014, **140**, 064505.
42 A. Klamt, *COSMO-RS from quantum chemistry to fluid phase thermodynamics and drug design*, Elsevier, Amsterdam, The Netherlands, 2005.
43 A. Klamt, *Wiley Interdiscip. Rev.: Comput. Mol. Sci.*, 2011, **1**, 699.
44 M. A. R. Martins, C. M. S. S. Neves, K. A. Kurnia, L. Andreia, L. M. N. B. F. Santos, M. G. Freire, S. P. Pinho and J. A. P. Coutinho, *Fluid Phase Equilib.*, 2014, **375**, 161.
45 M. G. Freire, C. M. S. S. Neves, S. P. M. Ventura, M. J. Pratas, I. M. Marrucho, J. Oliveira, J. A. P. Coutinho and A. M. Fernandes, *Fluid Phase Equilib.*, 2010, **294**, 234.
46 C. M. S. S. Neves, A. R. Rodrigues, K. A. Kurnia, J. M. S. S. Esperança, M. G. Freire and J. A. P. Coutinho, *Fluid Phase Equilib.*, 2013, **358**, 50.
47 G. Della Gatta, E. Badea and M. Saczuk, *J. Chem. Thermodyn.*, 2010, **42**, 1204.
48 K. Shimizu, C. E. S. Bernardes and J. N. Canongia Lopes, *J. Phys. Chem. B*, 2013, **118**, 567.
49 C. E. S. Bernardes, M. E. Minas da Piedade and J. N. Canongia Lopes, *J. Phys. Chem. B*, 2011, **115**, 2067.
50 M. A. A. Rocha, C. F. R. A. C. Lima, L. g. R. Gomes, B. Schröder, J. o. A. P. Coutinho, I. M. Marrucho, J. M. S. S. Esperança, L. s. P. N. Rebelo, K. Shimizu, J. N. Canongia Lopes and L. s. M. N. B. F. Santos, *J. Phys. Chem. B*, 2011, **115**, 10919.
51 S. P. M. Ventura, M. Gurbisz, M. Ghavre, F. M. M. Ferreira, F. Gonçalves, I. Beadham, B. Quilty, J. A. P. Coutinho and N. Gathergood, *ACS Sustainable Chem. Eng.*, 2013, **1**, 393.
52 C. M. S. S. Neves, M. L. S. Batista, A. F. M. Claudio, L. M. N. B. F. Santos, I. M. Marrucho, M. G. Freire and J. A. P. Coutinho, *J. Chem. Eng. Data*, 2010, **55**, 5065.
53 A. Klamt and F. Eckert, *Fluid Phase Equilib.*, 2000, **172**, 43.
54 A. Klamt, J. Reinisch, F. Eckert, A. Hellweg and M. Diedenhofen, *Phys. Chem. Chem. Phys.*, 2012, **14**, 955–963.
55 F. Eckert and A. Klamt, COSMOlogic GmbH & Co. KG, Leverkusen, Germany, 2013.
56 K. A. Kurnia and J. A. P. Coutinho, *Ind. Eng. Chem. Res.*, 2013, **52**, 13862.
57 M. G. Freire, S. P. M. Ventura, L. M. N. B. F. Santos, I. M. Marrucho and J. A. P. Coutinho, *Fluid Phase Equilib.*, 2008, **268**, 74.
58 W. Smith and T. R. Forester, *The DL_POLY Package of Molecular Simulation Routines (v.2.2) The Council for The Central Laboratory of Research Councils*, Daresbury Laboratory, Warrington, United Kingdom, 2006.
59 M. Praprotnik, D. Janežič and J. Mavri, *J. Phys. Chem. A*, 2004, **108**, 11056.
60 J. N. Canongia Lopes, J. Deschamps and A. A. H. Pádua, *J. Phys. Chem. B*, 2004, **108**, 2038.
61 J. N. Canongia Lopes and A. A. H. Pádua, *J. Phys. Chem. B*, 2004, **108**, 16893.
62 K. Shimizu, D. Almantariotis, M. F. C. Gomes, A. A. H. Pádua and J. N. Canongia Lopes, *J. Phys. Chem. B*, 2010, **114**, 3592.
63 W. L. Jorgensen, D. S. Maxwell and J. Tirado-Rives, *J. Am. Chem. Soc.*, 1996, **118**, 11225.
64 K. Shimizu, C. E. S. Bernardes, A. Triolo and J. N. Canongia Lopes, *Phys. Chem. Chem. Phys.*, 2013, **15**, 16256.
65 A. A. Freitas, K. Shimizu and J. N. Canongia Lopes, *J. Chem. Eng. Data*, 2014, DOI: 10.1021/je500197x, article ASAP.
66 Azur Environmental, MicrotoxOmniTM Software for Windows(r) 95/98/NT. 1999, Carlsbad, CA, U.S.A.